Optimum design of the cored linear motor using experiment design[†]

Sungill Seo and Naksoo Kim[*]

Department of Mechanical Engineering, Sogang University, Seoul, 121-742, Korea

---

Abstract

Recently, a linear motor has been becoming widely popular in office automation (OA) and factory automation (FA) systems due to its simple structure, high-speed operation, and precise positioning. In this study, a cored linear motor was designed to have a large thrust and small ripple because these are considered as indicators of motor performance. The thrust and ripple of the linear motor can be calculated by a finite element method (FEM) commercial program such as ANSYS. To design the cored linear motor, first, the design variables were selected through ANOM and ANOVA. The response surface method was applied to formulate the cost function of the second-order regression model, which can evaluate motor performance. By optimizing the cost function, it was possible to realize quickly the optimum design for a cored linear motor. As a result, the performance of the motor was improved.

Keywords: Cored linear synchronous motor; Table of orthogonal array; Analysis of means; Analysis of variance; Response surface methodology; Thrust force

---

1. Introduction

When we build a system using a rotator motor, mechanical transformation contrivances such as a screw, a chain, and a gear box are needed to convert a circle motion into a linear one. During this process, however, the energy efficiency is lowered because of energy loss from friction. To reduce energy loss, therefore, a linear motor that can produce linear motion can be used instead of a rotator motor. As a control tool of position and speed, a linear motor can provide fast speed, a powerful thrust, and a precise dynamic positioning [1, 2]. In fact, linear motors are used in factory automation, magnetic levitation trains, and semiconductor equipment, among others. Recently, their application has been extended to small precision products like hard disks and CD players.

Accordingly, there have been many studies on this type of motor, including theoretical thrust analysis, and on special quality improvement based on electromagnetic force analysis like the finite element method, equivalent magnetic circuit network method, and so on. In relation to this, Mizuno and Yamada (1999) studied the size effect of the permanent magnets in a linear synchronous motor because these magnets affect the static thrust and vertical force of the core [3]. Yamada (1996) found the solution to an optimization problem in order to maximize thrust under the constraints of the thickness of the linear motor and the values of the design parameters, namely, the number of turns of the coil and the thickness of the magnets [4]. Hong et al. (2006) studied the improvement of the thrust of a transverse flux linear motor by using the response surface method (RSM) [5]. Choi et al. (1999) used the size and material of a stator to increase gap magnetic flux density [6]. Some researchers were able to achieve improved thrust through the optimum design of the linear motor using a genetic algorithm [7-9].

The purpose of this study is to increase the thrust of the cored linear motor and make the motor cheaper than other linear motors through optimization of the

design considering the ripple. We set the design parameters and conduct experiments according to the experiment design in order to achieve the optimum design in a limited volume [10, 11]. Furthermore, we choose the design parameters by using ANOVA and ANOM. After using the response surface method and setting the cost function, the optimum design can be obtained through minimization of the cost function [12, 13].

2. Theory of the linear motor

2.1 Kinds of linear motor

A linear motor is basically a structure unfolding a rotator motor, as shown in Fig. 1. A linear motor can produce straight-line motion without the need for mechanical transformation devices for a system needing straight-line motion.

A linear motor may be classified as a linear step motor (LPM), linear induction motor (LIM), linear direct current motor (LDM), or linear synchronous motor (LSM) according to its characteristics [8]. LPM can operate without a permanent magnet and encoder, and it is also cheap, but it has a low thrust. LIM can produce a large thrust without a permanent magnet, but its calorific value is large, and it has low accuracy because it uses high electric current. LDM is supplied with electric current via a commutator and brush, like a DC motor, but its use is limited because it needs a better control technique. Lastly, LSM using a permanent magnet can produce high thrust, and it has high efficiency as well as a low calorific value [9]. LSM is classified further into the coreless type and the cored type. This study implements the optimum design of the cored LSM, which can produce thrust greater than the coreless LSM, by using a common FEM package.

2.2 FEM modeling

In this study, we used low-frequency electromagnetic analysis. Maxwell's equations are used as the governing equation. Eq. (1) shows Maxwell's equations in low-frequency electromagnetic state.
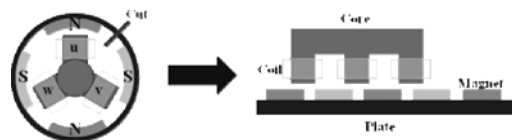

Fig. 1. The linear motor concept.

$$\nabla \times \mathbf{E} = -\frac{\partial \mathbf{B}}{\partial t} \qquad \nabla \times \mathbf{H} = \mathbf{J}$$
$$\nabla \bullet \mathbf{D} = \rho \qquad \nabla \bullet \mathbf{B} = 0 \qquad (1)$$

where $\mathbf{B}$ is the magnetic flux density, and $\mathbf{H}$ is the magnetic field intensity. $\mathbf{E}$ is the electric field intensity, and $\mathbf{D}$ is electric flux density. $\mathbf{J}$ is the current density, and ρ is the charge density.

The FEM simulation tool used to analyze the magnetic field is ANSYS. A basic model of a linear motor consists of a fixed stator, the permanent magnets arranged above the stator, and a moving core, which is wound by coils, as shown in Fig. 2. Table 1 lists the material of each part. Each leg of the core is wound with a coil of 190 turns and a flow of 3.8A electric current with a 120-degree phase difference.

When the core passes a permanent magnet N-S pole twice, this is one cycle. One cycle of the linear motor designed in this study is 60mm; the thickness

Table 1. Composition of the parts.

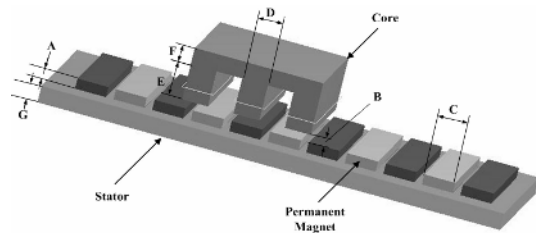| Stator	SS416
Core	Silicon Core Iron
Magnet	950 A/mm of Coercive Force 1.2 T of Residual Induction

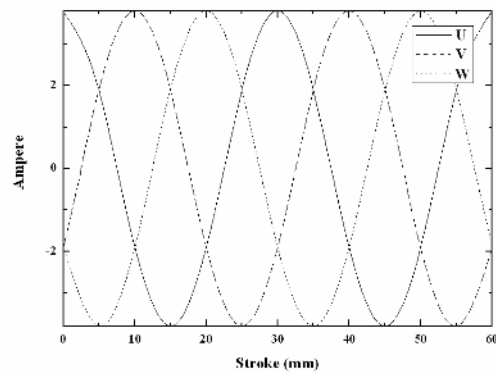Fig. 2. FEM model of the Cored Linear Motor and Design variables.

Fig. 3. Electric current value of the coil during one cycle.

of the permanent magnet is 50mm, while the thickness of the stator is 70mm. When a core moves 2.5mm, this is one step. The thrust is calculated by FEM simulation with 25 steps, during one cycle. Fig. 3 shows the change in electric current at U, V, and W during one cycle.
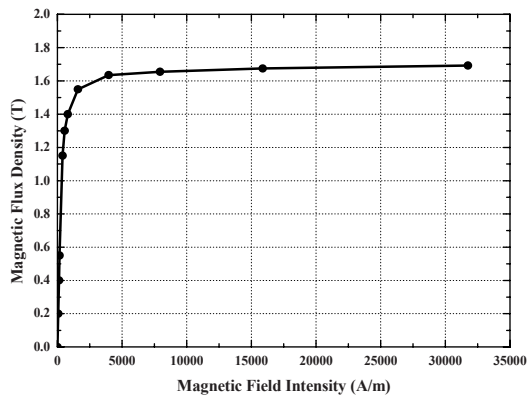
We performed 3-D nonlinear analysis. The number of elements is 90,498. Fig. 4 shows the B-H curves of the core and the stator.

Table 2 shows the initial values of the design parameters that are defined in Fig. 2. The simulation with these initial values shows a change in the phase of the thrust according to the position of the core, as shown in Fig. 5.
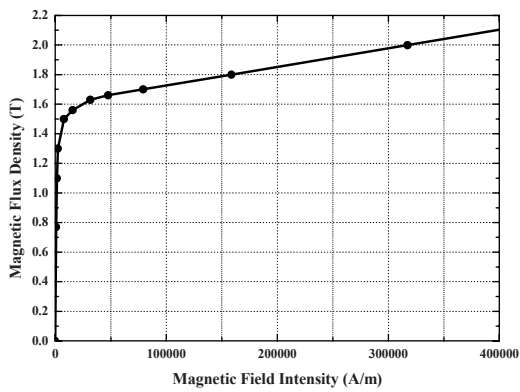
Fig. 5 shows that a thrust is not fixed by the position of the core, and it has a cycle. As a characteristic

Table 2. Initial design value (unit: mm).

A	B	C	D	E	F	G
3	1.5	12	10	13.5	6.5	6.5

(a)

(b)

Fig. 4. B-H curves of (a) the core and (b) the stator.

of the thrust, the ripple has to be considered in an optimum design. To express a ripple as a numerical value, a standard variation of thrust, which is calculated in Eq. (2) during one cycle, is used. The lower the ripple values are, the better the design is.

$$S = \sqrt{\sum_{x=1}^{n} \frac{(F_x - \overline{F})^2}{n}} \qquad (2)$$

2.3 Measurement of the thrust through an experiment

We have to confirm that the values calculated by the FEM simulation tool are reasonable to use. Therefore, we obtained the thrust of an existing linear motor by experiment and compared this with the thrust calculated by a simulation tool. A digital indicator and a load cell made by Sewoo Industrial System Co., as shown in Fig. 6, were used in the experiment.
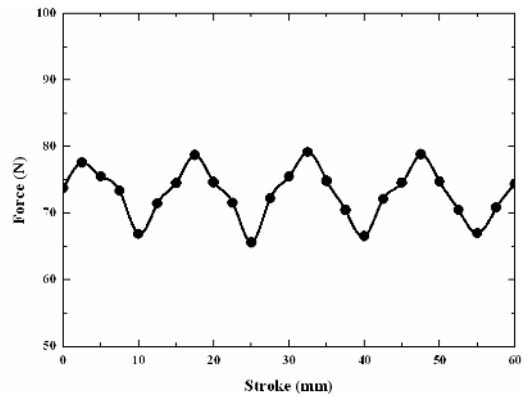

Fig. 5. Directional force of the core during one cycle using initial design values.

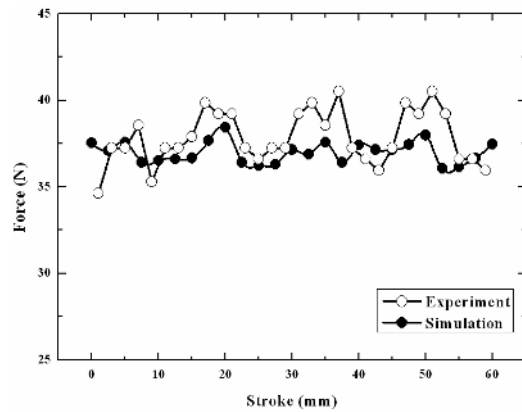Fig. 6. A digital indicator and a load cell.

Fig. 7. Comparison of thrusts between the experiment result and the FEM simulation result.

The thrust measurement method followed these procedures. First, a fixed amount of electric current is made to flow into the digital indicator. At that time, the motor should have a torque which pushes the push gauge. Finally, the load cell measures the thrust.

Fig. 7 shows the result of the experiment and the calculation. The calculated thrust by the FEM simulation tool is a little smaller than the thrust that was measured by the experiment. However, the pattern of the thrust is very similar between the experiment and the calculation. Therefore, it seems reasonable to calculate the thrust using the FEM simulation tool.

3. Experiment design using the table of orthogonal array

3.1 Constitution of the table of orthogonal array

The experiment design refers to the plan of experiments, including the method of setting up the experiment to solve a particular problem, the method of data collection, and the method of obtaining the most information by using the minimum number of experiments based on statistical data analysis [14]. Therefore, using the experiment design requires the selection of parameters about the problem, choice of an appropriate experimental method, decision on the experiment order, and selection of the optimum analysis method for the data obtained from the experiment.

In a general design, there are many parameters to be considered. The table of orthogonal array considers all parameters but excludes information about an interaction of a higher degree between parameters. Therefore, we can make a plan of experiments with a

Table 3. Levels of the design variables (unit: mm).

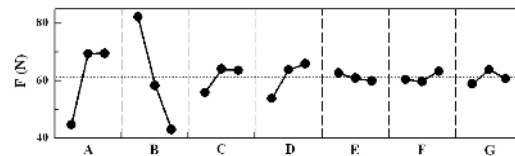| Design Variables	Level 1	Level 2	Level 3
A	1	3	5
B	0.5	1.5	2.5
C	9	12	15
D	5	10	15
E	10	13.5	17
F	4	6.5	9
G	3	6.5	10

Fig. 8. Illustration of the design variables' effect for thrust force.

small number. In the table of orthogonal array, many parameters can be included without an expansion of the experiment, and they can be used to easily calculate the effect of parameters from the experiment data. Moreover, we can employ ANOVA easily by using the table of orthogonal array.

In this study, the seven design parameters are set as shown in Fig. 2. Each parameter is classified into three levels. Table 3 shows the values of parameters according to the level. The table of orthogonal array is formed by using the mixing tables of the orthogonal array $L_{18}(2^1 \times 3^7)$, which disperses uniformly the interaction between the rows of parameters to other rows. Table 4 shows the composition of the table of orthogonal array, and the result of the simulation using ANSYS.

3.2 ANOM and ANOVA of the thrust

Based on the simulation result in Table 4, ANOM is carried out to determine the parameters that affect thrust. The larger the thrust is, the better the design is. Table 5 and Fig. 8 show the effect of levels of design variables and the variation of levels. The data show that design variables A, B, C, and D have a greater effect on thrust.

For quantitative analysis, the ANOVA of a thrust is carried out as shown in Table 6. The result shows that design variables A, B, C, and D have a greater effect on the thrust because the P values of the design variables A, B, C, and D are smaller than 0.05.

Table 4. Table of orthogonal arrays for the thrust and the ripple.

No.	A	B	C	D	E	F	G	Force (N)	Ripple
1	1	1	1	1	1	1	1	51.79	5.33
2	1	2	2	2	2	2	2	48.73	1.32
3	1	3	3	3	3	3	3	34.35	1.49
4	2	1	1	2	2	3	3	87.02	6.09
5	2	2	2	3	3	1	1	67.69	11.58
6	2	3	3	1	1	2	2	46.92	2.02
7	3	1	2	1	3	2	3	82.34	3.87
8	3	2	3	2	1	3	1	72.44	14.22
9	3	3	1	3	2	1	2	51.46	6.67
10	1	1	3	3	2	2	1	68.65	25.77
11	1	2	1	1	3	3	2	32.44	0.53
12	1	3	2	2	1	1	3	32.07	0.84
13	2	1	2	3	1	3	2	106.49	13.19
14	2	2	3	1	2	1	3	62.39	4.87
15	2	3	1	2	3	2	1	45.71	2.52
16	3	1	3	2	3	1	2	97.04	24.73
17	3	2	1	3	1	2	3	66.44	9.59
18	3	3	2	1	2	3	1	47.34	2.92

Table 5. Analysis of the means of thrust.

Design variables	Effect			Deviation	Percentage
	1	2	3		
A	44.67	69.37	69.51	14.30	28.08
B	82.22	58.35	42.98	19.78	38.83
C	55.81	64.11	63.63	4.66	9.15
D	53.87	63.84	65.85	6.42	12.60
E	62.69	60.93	59.93	1.40	2.75
F	60.41	59.80	63.35	1.90	3.73
G	58.94	63.85	60.77	2.48	4.87
Total				50.93	100

Table 6. Analysis of the variance of thrust.

Design variables	S	Φ	V	F0	P
A	2453.83	2	1226.92	114.95	0.001
B	4692.64	2	2346.32	219.83	0.001
C	260.48	2	130.24	12.20	0.036
D	493.84	2	246.92	23.13	0.015
E	23.49	2	11.75	1.10	0.438
F	43.26	2	21.63	2.03	0.277
G	73.92	2	36.96	3.46	0.166
Error	32.02	3	10.67		
Total	8073.49	17			

3.3 ANOM and ANOVA of the ripple

ANOM and ANOVA of the ripple were carried out as in the previous section. Unlike the thrust, the lower the ripple is, the better the design is.

Table 7 and Fig. 9 show the ANOM of the ripple. The result indicates that design variables A, B, C, D, and G have an effect on the thrust. However, as a result of ANOVA, only design variable B has a large effect on the ripple, as shown in Table 8.

Table 7. Analysis of the means of ripple.

Design variables	Effect			Deviation	Percentage
	1	2	3		
A	5.88	6.71	10.33	2.37	11.72
B	13.16	7.02	2.74	5.24	25.93
C	5.12	5.62	12.18	3.94	19.50
D	3.26	8.29	11.38	4.10	20.30
E	7.53	7.94	7.45	0.26	1.30
F	9.00	7.51	6.40	1.30	6.45
G	10.39	8.07	4.46	2.99	14.80
Total				20.20	100

Table 8. Analysis of the variance of ripple.

Design variables	S	Φ	V	F0	P
A	67.31	2	33.66	1.17	0.421
B	329.16	2	164.58	5.72	0.095
C	186.24	2	93.12	3.24	0.178
D	201.82	2	100.91	3.51	0.164
E	0.83	2	0.42	0.01	0.986
F	20.40	2	10.20	0.35	0.728
G	107.21	2	53.60	1.86	0.298
Error	86.32	3	28.77		
Total	999.29	17			

Table 9. Initial design value for the response surface method (unit: mm).

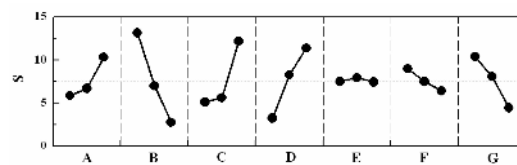| A	B	C	D	E	F	G
3	1.5	12	10	10	9	10

Fig. 9. Illustration of the design variables' effect for ripple.

3.4 Decision of the initial values for use in RSM

Generally, if the optimum design is achieved with ANOM and ANOVA, the design values are the specified values. However, since the numerical values of the design parameters are continuous, the specified values cannot yield a real optimum design. Therefore, as with the use of RSM which is carried out in the next section, this study provides an optimum design with other values in addition to the specified values. Before using RSM, the design variables affecting thrust and ripple should be determined from the results of analysis. Also, the initial design values that are close to the optimum design values are determined in order to obtain a more correct RSM [15]. If a multiplicity of variables is used, and the range of parameter levels is wide, the reliability of a cost function made by RSM would be low.

Based on the results presented in the previous section, the initial design values are obtained as in Table 9. In the same table, design variables E, F, and G, which have less effect, are fixed, while design variables A, B, C, and D are set up.

4. The response surface method

4.1 Constitution of RSM

RSM is a chain of processes that assume a relation between design variables and the response function as a mathematical equation, assume a coefficient of equation with the least square method from the measured data, and make a useful response surface model [16]. In this study, a second response surface model is used as given by Eq. (3).

$$y = \beta_0 + \sum_{i=1}^{n_d} \beta_i x_i + \sum_{i=1}^{n_d} \sum_{j \geq i}^{n_d} \beta_{ij} x_i x_j \tag{3}$$

where x_i are the design variables, n_d are the number of design variables, and β_i are the coefficients assumed by the least square method.

Eq. (4) is the calculation method of the coefficient of the response surface model.

$$\boldsymbol{\beta} = (\mathbf{X}^T \mathbf{X})^{-1} \mathbf{X}^T \mathbf{Y} \tag{4}$$

where $\mathbf{X}$ is a design matrix composed of experiment points, and $\mathbf{Y}$ is a response vector.

4.2 Application of RSM

To start using RSM, employing the initial design values found in the previous section, the experiment design is made again. The number of design variables is 4, and each variable has 3 levels, as shown in Table 10. On the basis of these data, a mixing table of an orthogonal array $L_{18}(2^1 \times 3^7)$ is made, as shown in Table 11. A thrust has a value between 50N and 100 N, and a ripple has a value between 1 and 8, so it is difficult to compare these two objectively. Therefore, these values are normalized by using Eq. (5) to lie between -1 and 1. The lower the normalized thrust is, the better the design is. Also, the lower the normalized ripple value is, the better the design is.

Table 10. Level of the design variables (unit: mm).

Design variables	Level -1	Level 0	Level 1
A	2	3	4
B	1	1.5	2
C	10.5	12	13.5
D	7.5	10	12.5

Table 11. Table of orthogonal arrays for the thrust and the ripple.

No.	A	B	C	D	Force	Ripple	Normalized force	Normalized ripple
1	-1	-1	-1	-1	70.37	5.18	-0.018	0.270
2	-1	0	0	0	66.33	2.00	0.183	-1
3	-1	1	1	1	59.14	3.14	0.543	-0.545
4	0	-1	0	1	90.16	6.41	-1.008	0.766
5	0	0	1	-1	71.39	4.55	-0.069	0.019
6	0	1	-1	0	59.00	2.67	0.550	-0.731
7	1	-1	1	0	93.14	7.12	-1.157	1.049
8	1	0	-1	1	73.34	6.72	-0.167	0.889
9	1	1	0	-1	63.52	3.35	0.324	-0.46
10	-1	-1	0	0	80.97	2.32	-0.549	-0.873
11	-1	0	1	1	70.72	3.87	-0.036	-0.252
12	-1	1	-1	-1	48.24	1.81	1.088	-1.075
13	0	-1	-1	1	83.45	5.76	-0.673	0.504
14	0	0	0	-1	70.00	2.83	0	-0.670
15	0	1	1	0	65.23	3.16	0.239	-0.536
16	1	-1	1	-1	86.36	7.24	-0.818	1.097
17	1	0	-1	0	72.17	4.60	-0.109	0.038
18	1	1	0	1	69.05	6.64	0.047	0.855

$$F_N = \frac{(70 - F)}{20}$$

$$S_N = \frac{(S - 4.5)}{2.5} \tag{5}$$

As a result of the simulation, the response surface of the thrust is given by Eq. (6), and the response surface of the ripple is given by Eq. (7).

$$
\begin{aligned}
f(\underline{x}) =\ & -0.203 - 0.269x_1 + 0.603x_2 - 0.195x_3 \\
& -0.141x_4 + 0.114x_1^2 - 0.102x_2^2 + 0.09x_3^2 \\
& +0.067x_4^2 - 0.02x_1x_2 + 0.034x_1x_3 - 0.032x_1x_4 \\
& +0.032x_2x_3 + 0.037x_2x_4 - 0.039x_3x_4
\end{aligned} \tag{6}
$$

$$
\begin{aligned}
r(\underline{x}) =\ & -4.89 + 6.26x_1 - 3.83x_2 + 1.27x_3 \\
& +4.18x_4 - 0.13x_1^2 - 0.82x_2^2 + 3.16x_3^2 \\
& +4.58x_4^2 + 0.83x_1x_2 + 3.3x_1x_3 + 1.29x_1x_4 \\
& +0.01x_2x_3 + 1.47x_2x_4 + 0.94x_3x_4
\end{aligned} \tag{7}
$$

where $\underline{x}$ are normalized design variables, and A, B, C, D and are calculated by Eq. (8).

$$x_1 = A - 3 \qquad x_2 = 2B - 3$$

$$x_3 = \frac{2}{3}C - 8 \qquad x_4 = 0.4D - 4 \tag{8}$$

5. Optimum design

5.1 Setting a cost function

Using the response surface functions of thrust and the ripple calculated in the previous section, a cost function of the linear motor is made. A cost function is the summations of the response surface functions of thrust and ripple because these two are normalized to have a value between -1 and 1. Then we give a weight to each function by multiplying a coefficient like Eq. (9). The effect of the thrust is bigger than that of the ripple in the optimum design, so weight *a* is set as 2 and *b* is set as 1. By applying constraints, the optimum design does not lean to any one side, thrust, or ripple [17].

$$
\begin{aligned}
\text{Minimize} \quad & c(\underline{x}) = a \times f(\underline{x}) + b \times r(\underline{x}) \\
\text{Subject to} \quad & -2 < x_1 < 2 \qquad -2 < x_2 < 2 \\
& -2 < x_3 < 2 \qquad -2 < x_4 < 2 \\
& f(\underline{x}) < 0.5 \qquad r(\underline{x}) < 0.5
\end{aligned} \tag{9}
$$

5.2 Optimization of the cost function

The cost function calculated in the previous section is optimized. The BFGS and SUMT methods using the inverse barrier function are used as the optimum techniques. Table 12 shows the optimum values. Then using the optimum design values, the simulation is conducted again. Table 13 presents the simulation results, which are similar to those obtained by using the cost function.

Table 14 and Fig. 10 compare the thrust and ripple between the initial design and the optimum design. The average thrust of the optimum design was 32% higher than that of the initial design. However, the

Table 12. Calculated design values.

Design variables	Transformed values	Optimum values (mm)
A	-0.1539	2.85
B	-1.5	0.75
C	0.2818	12.42
D	-0.039	9.9

Table 13. Comparison of results between the simulation and the response surface method.

	Cost function	Simulation	Error (%)
Thrust (N)	97.04	96.05	1.03
Ripple	4.15	4.25	2.35

Table 14. Comparison of results between the simulation and the response surface method.

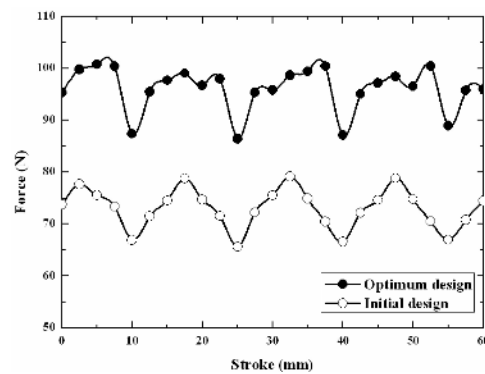|	Initial	simulation	Difference (%)
Thrust (N)	73.01	96.05	31.55
Ripple	3.81	4.05	6.30

Fig. 10. Comparison of the directional force of the core during one cycle.

ripple of the optimum design increased by 6%. This is because the weight of the response surface function of the thrust is bigger than that of the ripple. Therefore, the motor is designed to have a large thrust. As a result, the summation of the normalized thrust and ripple by using the optimum values with weights was lower than the summation of the normalized thrust and ripple obtained by using the initial values.

6. Conclusions

In this study, a shape of the cored linear motor was chosen in a limited volume. The height of the stator, the height and length of the permanent magnet, the height and thickness of the core, and the gap between the core and the permanent magnet were selected as the design variables.

To obtain an efficient design, the table of orthogonal array was used. We derived similar results by using a full factorial experiment with the minimum numbers of simulation. The design variables that affect the thrust and ripple can be found through ANOVA and ANOM.

We also constituted the table of orthogonal array to have levels within narrow limits. By doing so, the response surface model can be constituted with design values that are close to the optimum values, and the cost function can be formulated more accurately than the response surface function without the need for previous studies in order to determine the initial design values.

A cost function has to consider both the thrust the ripple. Therefore, the cost function was constituted with the use of a weight for the thrust and the ripple. With this method, the designer can obtain the optimum result he/she originally wanted. In this study, we gave a weight rate of 2:1 in order to obtain a bigger thrust effect. The average thrust also increased by 32% as compared to that using the initial design values through the optimum method.

In this study, the optimum design of the cored linear motor is made by using fast FEM simulation with an upgraded computer and the minimum simulation numbers through experiment design. With the use of the same process, other linear motors can be designed easily in addition to the cored linear motor.

References

[1] K. J. Binns, Permanent magnet AC generators, *Proc.*

IEEE, 126 (7) (1979) 690-696.

[2] T. Alasuvanto, Comparison of Four Different Permanent Magnet Rotor Constructions, *Int. Conf. On Electrical Machines*, (1990) 1034-1039.

[3] T. Mizuno and H. Yamada, Magnet Circuit Analysis of a Linear Synchronous Motor with Permanent Magnets, *IEEE Trans*. On Magn., 14, (4) (1999) 3027-3029.

[4] H. Yamada, Optimum Design of Thin Linear DC Motor with Long Strokes, *T.IEE Japan*, 116-D (4) (1996) 348-389.

[5] D. K. Hong, B. C. Woo and D. H. Kang, Optimal Geometric Design of Transverse Flux Linear Motor Using Response Surface Methodology, *Trans. KIEE*, 55B (10) (2006) 498-504.

[6] M. S. Choi, Y. Y. Kim and S. L. Lee, The Optimum Geometric Design Stators for a Brushless DC Linear Motor, *Trans. KSME*, A, 23 (3) (1999) 442-448.

[7] S. H. Joo, J. H. Jung and S. R. Lee, A Study on Optimization of the Design Variables of Linear Motor Using Genetic Algorithm, *J. of KSPE*, 19 (5) (2002) 110-117.

[8] J. H. Jung, S. H. Shin and S. R. Lee, Optimization of the Design Variables of Linear Motor by FEM, *Trans. KSME*, A, 26 (7) (2002) 1232-1240.

[9] I. U. Eun, Improvement of the Thermal Characteristics of Synchronous Linear Motors Through Insulation, *J. of KSPE*, 19 (3) (2002) 123-130.

[10] D. K. Hong, B. C Woo and D. H. Kang, Optimum Design of Transverse Flux linear Motor for Maximizing Thrust Force using Table of Orthogonal Array, *Trans. KIEE*, 54B (11) (2005) 505-510.

[11] E. S. Kim, I. S. Lee and B. M. Kim, Optimum Design of Washing Machine Flange using Design of Experiment, *Trans. KSME*, 31 (5) (2007) 601-608.

[12] H. Kurtaran, A. Eskandarian, D. Marzougui and N. E. Bedewi, Crashworthiness Design Optimization using Successive Response Surface Approximations, *Computational Mechanics*, 29 (2002) 409-421.

[13] W. Roux, N. Stander and R. Haftka, Response Surface Approximations for Structural Optimization, *Int. J. Numer. Methods Eng.*, 42 (1998) 517-534.

[14] J. M. Lim, S. Han, S. Jeon, D. Woo and G. J. Park, Analysis and Design Considerations of Energy Absorbing Steering System using Orthogonal Arrays, *Trans. KSAE*, 7 (6) (1999) 144-155.

[15] T. H. Lee, J. J. Jung, S. Hong, H. W. Kim and J. S. Choi, Statistical Analysis and Prediction for Behav-

iors of Tracked Vehicle Traveling on Soft Soil Using Response Surface Methodology, *Trans. KSOE*, 20 (3) (2006) 54-60.

[16] B. D. Youn and K. K. Choi, A new Response Surface Methodology for Reliability Based Design Optimization, *Computers and Structures*, 82 (2) (2004) 241-256.

[17] Y. Y. Kim, S. J. Heo, M. S. Kim, I. K. Jun and J. M. Choi, Multi-Criteria Optimization for Dynamic Load Reduction of Passenger Car Suspension System, *Trans. KSAE* (2006) 703-708.

Mr. Sungill Seo received his B.S. and M.S. degree from the department of Mechanical Engineering, Sogang University, Seoul, S. Korea in 2006 and 2009, respectively. Mr. Seo is currently working for Hyundai Engineering. His research interests are in the area of optimum design of electric motors, metal forming, and process design.

Naksoo Kim received his B.S. and M.S. degree from the department of Mechanical Design, Seoul National Uni-versity in 1982 and 1984, respectively. He then went on to receive his Ph. D. degree from U.C. Berkeley. Dr. Kim had worked for the ERC/NSM at the Ohio State University as a senior researcher and Hongik University as an assistant professor. He is currently a professor at the department of mechanical engineering, Sogang University. Dr. Kim's research interests are in the area of metal forming plasticity, computer aided process analysis, and optimal design.